



# Understanding coastal wetland conditions and futures by closing their hydrologic balance: the case of the Gialova lagoon, Greece

Stefano Manzoni<sup>1,2</sup>, Giorgos Maneas<sup>1,3</sup>, Anna Scaini<sup>1,2</sup>, Basil E. Psiloglou<sup>4</sup>, Georgia Destouni<sup>1,2</sup>, and Steve W. Lyon<sup>1,2,5,6</sup>

<sup>1</sup>Department of Physical Geography, Stockholm University, 10691 Stockholm, Sweden

<sup>2</sup>Bolin Centre for Climate Research, Stockholm University, 10691 Stockholm, Sweden

<sup>3</sup>Navarino Environmental Observatory, 24001, Messinia, Greece

<sup>4</sup>Institute for Environmental Research & Sustainable Development, National Observatory of Athens, 15236, Athens, Greece

<sup>5</sup>The Nature Conservancy, 08314 Delmont, New Jersey, USA

<sup>6</sup>School of Environment and Natural Resources, Ohio State University, 43210 Columbus, Ohio, USA

**Correspondence:** Stefano Manzoni (stefano.manzoni@natgeo.su.se)

Received: 22 July 2019 – Discussion started: 19 August 2019

Revised: 27 April 2020 – Accepted: 12 June 2020 – Published:

**Abstract.** Coastal wetlands and lagoons are under pressure due to competing demands for freshwater resources and climatic changes, which may increase salinity and cause a loss of ecological functions. These pressures are particularly high in Mediterranean regions with high evaporative demand compared to precipitation. To manage such wetlands and maximize their provision of ecosystem services, their hydrologic balance must be quantified. However, multiple channels, diffuse surface water exchanges, and diverse groundwater pathways complicate the quantification of different water balance components. To overcome this difficulty, we developed a mass balance approach based on coupled water and salt balance equations to estimate currently unknown water exchange fluxes through the Gialova lagoon, southwestern Peloponnese, Greece. Our approach facilitates quantification of both saline and freshwater exchange fluxes, using measured precipitation, water depth and salinity, and estimated evaporation rates over a study period of 2 years (2016–2017). While water exchanges were dominated by evaporation and saline water inputs from the sea during the summer, precipitation and freshwater inputs were more important during the winter. About 40 % and 60 % of the freshwater inputs were from precipitation and lateral freshwater flows, respectively. Approximately 70 % of the outputs was due to evaporation, with the remaining 30 % being water flow from the lagoon to the sea. Under future drier and warmer conditions, salinity in the lagoon is expected to increase, unless freshwa-

ter inputs are enhanced by restoring hydrologic connectivity between the lagoon and the surrounding freshwater bodies. This restoration strategy would be fundamental to stabilizing the current wide seasonal fluctuations in salinity and maintain ecosystem functionality but could be challenging to implement due to expected reductions in water availability in the freshwater bodies supporting the lagoon.

## 1 Introduction

Coastal wetlands and lagoons regulate hydrologic, sediment, and contaminant exchanges between inland water bodies and the sea; they sustain biodiverse and highly productive ecosystems and provide important ecosystem services (Thorslund et al., 2017; Newton et al., 2014). The maintenance of these essential functions is threatened by competing demands and climatic changes. Reduced freshwater inflows due to intensified water use in upstream catchments, drainage efforts to convert wetlands to agricultural areas, and construction of infrastructure that interferes with the natural water flows are all causes of reduced wetland functionality from both ecological and human perspectives (e.g., Jaramillo et al., 2018; Newton et al., 2014). In regions with high population density and therefore a higher risk of wetland overexploitation, these anthropogenic changes are compounded with ongoing climatic trends, resulting in lower precipitation and higher

evaporation rates. These trends are expected to continue and possibly worsen as global temperatures rise.

Mediterranean lagoons in particular are under pressure due to competing demands for water resources from agriculture, tourism, the fish industry and ecological systems relying on lagoons for their survival (Maneas et al., 2019; Perez-Ruzafa et al., 2011). While runoff is already decreasing in this region (e.g., Destouni and Prieto, 2018), climatic changes are expected to increase aridity by lowering the difference between precipitation and potential evapotranspiration by as much as  $2\text{--}4\text{ mm d}^{-1}$  on an annual basis (Gao and Giorgi, 2008; Cheval et al., 2017). Therefore, coastal areas in the Mediterranean region (and wetlands in particular) are regarded as vulnerable to climatic changes (Klein et al., 2015; Gao and Giorgi, 2008).

To study the consequences of changing hydrologic regimes on wetlands (in terms of water quantity and quality), it is necessary to quantify hydrologic fluxes. This is generally difficult due to the complex land–water interactions in wetlands, and compound interactions of land and sea with lagoon water bodies. The lack of monitoring data for these multiple pathways of water exchange makes the prediction of hydrologic changes challenging, requiring indirect approaches that leverage the limited available data. To this end, overarching mass balance considerations and closure over a whole lake or wetland system can help constrain unknown fluxes of water, solutes and latent heat (Destouni et al., 2010; Jarsjo and Destouni, 2004; Assouline, 1993). Previous examples have also demonstrated the advantage of this approach for coastal lagoons (Martinez-Alvarez et al., 2011; Rodellas et al., 2018). In this contribution, we develop this approach and describe a minimal coupled water–salt mass balance model to determine both freshwater and saline flux exchanges of coastal water bodies.

While this approach is general, we focus its application on the Gialova lagoon (southwestern Peloponnese, Greece), the center of a Natura2000 protected area with a long history of water resource management that has radically altered the lagoon functioning (Maneas et al., 2019). This hydrologic system, characterized by unquantified point and diffuse water exchanges between lagoon and inland freshwater bodies, and between the lagoon and the Ionian Sea, offers an opportunity to apply the mass balance approach to estimate unknown hydrologic fluxes. Specifically, we start by quantifying freshwater and saline water exchange rates over a period of 2 years, to evaluate the Gialova lagoon water balance for the study period. Second, we use the results obtained for current climatic conditions and in scenarios of altered precipitation, evaporation rate, and freshwater inputs to assess how climatic changes and water management may alter the lagoon salinity, used here as a proxy for its ecological status.

## 2 Methods

### 2.1 Study area and climatic conditions

The Gialova lagoon is located in southwestern Messinia, Greece ( $36.97^\circ\text{ N}$ ,  $21.65^\circ\text{ E}$ ; Fig. 1a). The main water body of the lagoon, on which this contribution focuses, covers an area of a 225.5 ha; an additional 85.2 ha is covered by surrounding wetland areas (Maneas et al., 2019). The spatial average of water depth in the main water body is approximately 0.6 m, with a range between 0.27 and 0.77 m (Dounas and Koutsoubas, 1996). The lagoon is delimited by sand barriers formed around 5000 yr BP (Emmanouilidis et al., 2018), which separate the lagoon from Navarino Bay to the south and Voidokilia Bay to the northwest. It is reasonable to assume that groundwater exchanges occur through these relatively narrow sand barriers; in addition, a permanently open canal connects the Gialova lagoon to Navarino Bay. The Palaiokastro hill delimits the lagoon on the west side, whereas on the north the lagoon is separated from agricultural areas by a canal built in 1960 to divert water from the Xerolagados River directly to Voidokilia Bay. On the east and southeast sides, wetland areas surround the main lagoon water body. The Tyflomitis artesian springs provide freshwater to this area, thanks to freshwater aquifers feeding them from the east (Pantazis, 2019). Historically, the flow from these springs was approximately  $\approx 1.6 \times 10^6\text{ m}^3\text{ yr}^{-1}$ , but under current conditions it is limited to  $\approx 5 \times 10^5\text{ m}^3\text{ yr}^{-1}$  due to water extraction upstream (Maneas et al., 2019). Furthermore, only an unknown fraction of this flow enters the wetlands and lagoon, through up-welling and surface freshwater bodies, due to a diversion canal carrying most of the spring water to Navarino Bay. On the north side, the canal draining the Xerolagados river is currently not connected with the lagoon, but groundwater from the alluvial plain probably contributes freshwater to the lagoon, at least during the wet season. However, this aquifer is prone to salt intrusion from the Gialova lagoon during the dry season (Pantazis, 2019).

The area is characterized by a Mediterranean climate, with mild wet winters and dry summers (Fig. 1b and c). The mean annual temperature is  $18^\circ\text{ C}$  and the mean annual precipitation is  $695\text{ mm yr}^{-1}$  (measured from 1956 to 2011 at the Hellenic National Meteorological Service's station of Methoni, 15.6 km south of the Gialova lagoon (Hellenic National Meteorological Service, personal communication, 2019)). Trends in temperature and precipitation over the measurement period are weak and not statistically significant. The mean annual potential evapotranspiration has been estimated with the Thornthwaite method to be  $889\text{ mm yr}^{-1}$  (Maneas et al., 2019). Seasonal patterns are clear in all these hydroclimatic variables, with dry and hot summers and wet and mild winters. Precipitation shows higher variability than temperature and potential evapotranspiration, as indicated by larger differences between the 5th and 95th percentiles of the monthly values (shaded areas in Fig. 1b and c).

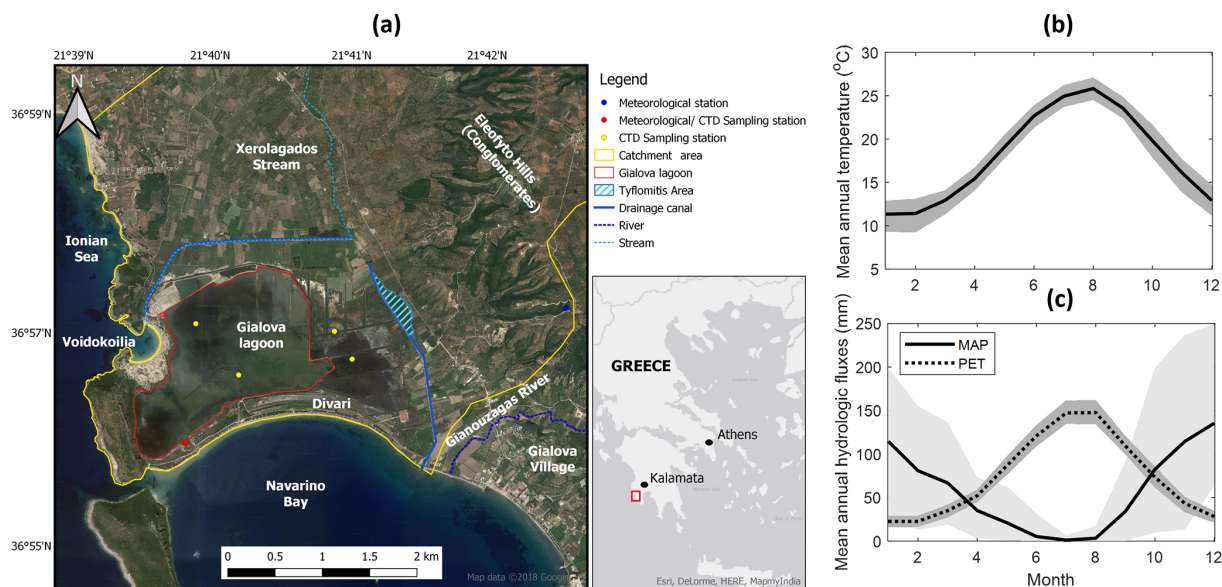


**Figure 1.** (a) Map of the study area; (b) long-term mean annual temperature; (c) long-term mean annual precipitation (MAP) and potential evapotranspiration (PET). In (b) and (c), shaded areas indicate the variability around the mean (5th and 95th percentiles). Sources for (a): AeroGRID, CNES/Airbus DS, DigitalGlobe, Earthstar Geographics, Esri, Garmin, GeoEye, GIS user community, HERE, IGN, © OpenStreetMap contributors 2019 (distributed under a Creative Commons BY-SA License), USDA, USGS.

## 2.2 Theory

Balance equations are formulated for both water volume and salt mass in the Gialova lagoon. The lagoon receives freshwater inputs from precipitation and both surface water and groundwater fluxes, and saline water from the Navarino and Voidokilia bays (collectively referred to as “sea” in the following). Outputs include evaporation and water discharge to the sea. Salt is exchanged with the sea (input or output depending on flow direction), and the salt exchange fluxes depend on both the water fluxes and the salinity of the source water body. All water exchanges, except precipitation (measured) and evaporation rate (modeled based on local meteorological data), are regarded as unknown. For convenience, water and salt fluxes are defined as positive when entering the lagoon. Water fluxes are expressed as volume per unit area of the lagoon and time (e.g.,  $\text{mm d}^{-1}$ ) and salt mass fluxes as mass per unit area and time (e.g.,  $\text{g m}^{-2} \text{d}^{-1}$ ); concentrations are expressed as mass per unit volume of water (e.g.,  $\text{g L}^{-1}$ ). Subscript “G” indicates the Gialova lagoon; subscript “S” indicates sea water. Symbols are listed and defined in Table 1.

### 2.2.1 Water balance equation

An overarching balance equation for water volume, neglecting water density variations, can be formulated for the lagoon in terms of its average water depth and the main water fluxes that regulate it as

$$\frac{1}{A} \frac{dV}{dt} = \frac{dh}{dt} = P - E + Q_{\text{fresh}} + Q_{\text{salt}}, \quad (1)$$

where  $A$  is the average surface area of the lagoon,  $h$  is the water depth in the lagoon,  $P$  and  $E$  are the rates of precipitation into and evaporation from the lagoon, respectively, and  $Q_{\text{fresh}}$  and  $Q_{\text{salt}}$  are the exchange rates of lateral freshwater and saline water fluxes into and from the lagoon (volumetric flow rates normalized by the lagoon area  $A$ ). This formulation rests on the assumption that variation and potential trends in water level are small, so that they do not significantly alter the extent of the lagoon area, which can then be sufficiently well represented by the average area  $A$  over the study period. This assumption is reasonable because the shoreline is mostly limited by man-made constructions with steep walls; only at the northwest side of the lagoon is a small area seasonally flooded. Assuming essentially constant lagoon area, changes in volume ( $V = hA$ ) can be approximated as  $A$  times the changes in water depth ( $\frac{dV}{dt} \approx A \frac{dh}{dt}$ ), justifying the first equality in Eq. (1).

In Eq. (1), precipitation rate and water depth are measured, while evaporation is estimated using the Penman equation, parameterized with local meteorological data (Sect. 2.2.3). The two remaining water fluxes,  $Q_{\text{fresh}}$  and  $Q_{\text{salt}}$ , are unknown and therefore solved for. A second equation is then necessary to obtain the two unknowns at each time step; this additional equality is provided by the salt balance.

**Table 1.** Definition of symbols used in the mass balance model and in the calculation of the evapotranspiration rate.

Symbol	Description	Units
Water and salt balance model (Eqs. 1–6)		
$A$	Gialova lagoon area	$\text{m}^2$
$C_G$	Salt concentration in the Gialova lagoon	$\text{g L}^{-1}$
$C_S$	Salt concentration in the Ionian Sea ( $= 38.5 \text{ g L}^{-1}$ )	$\text{g L}^{-1}$
$E$	Evaporation rate	$\text{mm d}^{-1}$
$F$	Salt mass exchange rate	$\text{g m}^{-2} \text{ d}^{-1}$
$h$	Gialova lagoon water depth	$\text{mm}$
$M$	Salt mass per unit area in the Gialova lagoon	$\text{g m}^{-2}$
$P$	Precipitation rate	$\text{mm d}^{-1}$
$Q_{\text{fresh}}$	Freshwater exchange rate (including surface and groundwater)	$\text{mm d}^{-1}$
$Q_{\text{salt}}$	Saltwater exchange rate (including surface and groundwater)	$\text{mm d}^{-1}$
$V$	Water volume in the Gialova lagoon	$\text{m}^3$
Runoff model (Eq. 12)		
AET	Actual evapotranspiration	$\text{mm yr}^{-1}$
PET	Potential evapotranspiration	$\text{mm yr}^{-1}$
$R$	Runoff from catchments surrounding the Gialova lagoon	$\text{mm yr}^{-1}$
Evaporation model (Eq. 7)		
$c_p$	Heat capacity of air	$\text{MJ kg}^{-1} \text{ }^\circ\text{C}^{-1}$
$e_s$	Saturated atmospheric vapor pressure	$\text{kPa}$
$e_a$	Actual atmospheric vapor pressure	$\text{kPa}$
$G$	Heat flow in the water column	$\text{MJ m}^{-2} \text{ d}^{-1}$
$r_a$	Aerodynamic resistance	$\text{d m}^{-1}$
$R_n$	Net radiation	$\text{MJ m}^{-2} \text{ d}^{-1}$
$\Delta$	Slope of the vapor pressure saturation-temperature relation	$\text{kPa } ^\circ\text{C}^{-1}$
$\gamma$	Psychrometric constant	$\text{kPa } ^\circ\text{C}^{-1}$
$\lambda$	Latent heat of vaporization	$\text{MJ kg}^{-1}$
$\rho_a$	Air density	$\text{kg m}^{-3}$
$\rho_w$	Water density	$\text{kg m}^{-3}$

### 2.2.2 Salt balance equation

The balance equation for the mass of salt, expressed in terms of salt mass per unit area of the lagoon reads

$$\frac{dM}{dt} = F, \tag{2}$$

where  $M$  is the salt mass per unit area (in  $\text{g m}^{-2}$ ) and  $F$  is the salt exchange rate per unit area (in  $\text{g m}^{-2} \text{ d}^{-1}$ ). Salt inputs via precipitation and atmospheric deposition are neglected (as in Obrador et al., 2008, for example). Following the above notations for water variables and assuming that waterborne salt transport is purely advective, the total salt mass and salt exchange rate can be calculated as

$$M = C_G h, \tag{3}$$

$$F = \begin{cases} C_G Q_{\text{salt}} & Q_{\text{salt}} < 0 \\ C_S Q_{\text{salt}} & Q_{\text{salt}} > 0 \end{cases} \tag{4}$$

In Eq. (3), the salt mass is obtained as the product of salt concentration ( $C_G$ ) and water depth ( $h$ ) in the Gialova lagoon. In

Eq. (4),  $Q_{\text{salt}}$  is still unknown, whereas  $C_G$  is measured and the seawater salinity  $C_S$  is assumed to be constant and equal to  $38.5 \text{ g L}^{-1}$  (Sect. 2.3.3). With this formulation, saline inputs through runoff are neglected. While this assumption is not always justified (Obrador et al., 2008), in the case of the Gialova lagoon, the intense water exchanges with Navarino Bay likely contribute more than inland sources to the salt budget.

Summarizing, we have now two equations in two unknowns (i.e.,  $Q_{\text{fresh}}$  and  $Q_{\text{salt}}$ ):

$$\frac{dh}{dt} = P - E + Q_{\text{fresh}} + Q_{\text{salt}}, \tag{5}$$

$$\frac{d(C_G h)}{dt} = \begin{cases} C_G Q_{\text{salt}} & Q_{\text{salt}} < 0 \\ C_S Q_{\text{salt}} & Q_{\text{salt}} > 0 \end{cases} \tag{6}$$

This system of equations is solved numerically using the finite difference method (Sect. 2.2.4), yielding the unknown freshwater and saltwater exchange rates. There are uncertainties associated with almost all fluxes and compartments,

but mathematically the problem is “closed” – that is, there is enough information to obtain both  $Q_{\text{fresh}}$  and  $Q_{\text{salt}}$ . Both mass balance equations are solved with a daily time resolution, but the results are aggregated to the monthly scale and over the whole study period.

### 2.2.3 Evaporation rate

The evaporation rate ( $E$ , expressed in  $\text{mm d}^{-1}$ ) is calculated using the Penman equation, parameterized following Duan and Bastiaanssen (2017),

$$E = \frac{1000}{\lambda \rho_w} \left[ \frac{\Delta}{\Delta + \gamma} (R_n - G) + \frac{\rho_a c_p}{\Delta + \gamma} \frac{e_s - e_a}{r_a} \right], \quad (7)$$

where all symbols are listed in Table 1 and the factor 1000 converts units from meters per day ( $\text{m d}^{-1}$ ) to millimeters per day ( $\text{mm d}^{-1}$ ).

To use Eq. (7) with the available data (Sect. 2.3), several assumptions are made. First, at the daily timescale, the contribution of heat flow in the lagoon ( $G$ ) is neglected. Second, net radiation ( $R_n$ ) is calculated as the difference between incoming shortwave plus longwave radiation, and outgoing shortwave plus longwave radiation, of which only incoming shortwave radiation is measured. Reflected shortwave radiation is estimated assuming an albedo of water equal to 0.08 (McMahon et al., 2013). Net outgoing longwave radiation is estimated using an empirical relation that accounts for both surface temperature and atmospheric conditions that affect incoming longwave radiation (Allen et al., 1998). In this relation, increasing vapor pressure and decreasing solar radiation (both quantities are measured at our site) decrease outgoing longwave radiation for a given surface temperature. Third, the aerodynamic resistance is parameterized for open-water evaporation following Shuttleworth (2012). To test this parameterization, the ratio of equilibrium evaporation and total evaporation was computed, resulting in a median value of 1.35 (first and third quartiles: 1.21 and 1.62, respectively). While this median value is higher than the classical result by Priestley and Taylor (1972) for wet vegetated surfaces (i.e., 1.26), our values are well within the range estimated for waterbodies (Assouline et al., 2016). This result thus lends support to the adopted parameterization. Finally, and similar to other studies using the Penman approach to estimate evaporation rate (e.g., Rosenberry et al., 2007; Martinez-Alvarez et al., 2011; Rodellas et al., 2018), we assume that conditions over the lagoon are homogeneous, and that our point measurements are representative. Considering the relatively small size of the lagoon, this assumption is deemed reasonable.

### 2.2.4 Numerical approach to solve the balance equations

The known quantities in Eqs. (5) and (6) include  $P$ ,  $C_G$ , and changes in water depth ( $\frac{dh}{dt} \approx \frac{\Delta h}{\Delta t}$  over a fixed, not infinitesimal, time interval), and  $E$  is estimated as described in

Sect. 2.2.3. To proceed,  $Q_{\text{fresh}}$  and  $Q_{\text{salt}}$  in Eqs. (5) and (6) must be expressed as functions of these known quantities. Equation (6) allows  $Q_{\text{salt}}$  to be found through

$$Q_{\text{salt}} = \begin{cases} \frac{1}{C_G} \frac{d(C_G h)}{dt} & Q_{\text{salt}} < 0 \\ \frac{1}{C_S} \frac{d(C_S h)}{dt} & Q_{\text{salt}} > 0 \end{cases}. \quad (8)$$

Using the chain rule of differentiation and discretizing through time, we obtain

$$\frac{d(C_G h)}{dt} = h \frac{dC_G}{dt} + C_G \frac{dh}{dt} \approx h \frac{\Delta C_G}{\Delta t} + C_G \frac{\Delta h}{\Delta t}, \quad (9)$$

where  $\Delta t$  is the discretization time step. If  $h \frac{\Delta C_G}{\Delta t} + C_G \frac{\Delta h}{\Delta t} > 0$ , salt mass increases and it follows that  $Q_{\text{salt}} > 0$ , so that the second expression in Eq. (8) is used to obtain  $Q_{\text{salt}}$ . In contrast, if  $h \frac{\Delta C_G}{\Delta t} + C_G \frac{\Delta h}{\Delta t} < 0$ , salt mass decreases and the first equation is used. Therefore, combining Eqs. (8) and (9), we finally obtain

$$Q_{\text{salt}} = \begin{cases} \frac{1}{C_G} \left( h \frac{\Delta C_G}{\Delta t} + C_G \frac{\Delta h}{\Delta t} \right), & h \frac{\Delta C_G}{\Delta t} + C_G \frac{\Delta h}{\Delta t} < 0 \\ \frac{1}{C_S} \left( h \frac{\Delta C_G}{\Delta t} + C_G \frac{\Delta h}{\Delta t} \right), & h \frac{\Delta C_G}{\Delta t} + C_G \frac{\Delta h}{\Delta t} > 0 \end{cases}. \quad (10)$$

The next step requires discretizing and solving Eq. (5) to obtain  $Q_{\text{fresh}}$  from the other hydrologic fluxes, changes in water depth, and  $Q_{\text{salt}}$  from Eq. (10),

$$Q_{\text{fresh}} = \frac{dh}{dt} - P + E - Q_{\text{salt}} \approx \frac{\Delta h}{\Delta t} - P + E - Q_{\text{salt}}. \quad (11)$$

The two linked Eqs. (10) and (11) do not need to be coupled through time because changes in water depth (though not water depth per se) and salt concentration in the lagoon are measured. These equations could thus be solved for each time interval in sequence. Since the value of water depth  $h$  varies from one time step to the next, and it is not measured,  $h$  in Eq. (10) must be updated at each time step as  $h_{t+1} = h_t + \Delta h$  before being entered in the equation for the next time step. This requires setting the initial value of water depth for this recursive calculation to start. As long as  $\Delta h/h \ll 1$ , this step would not be necessary, but since water depth fluctuations can be significant with respect to the mean depth in the shallow Gialova lagoon, this correction is important.

To summarize, Eqs. (10) and (11) represent a simple algorithm to calculate the unknown exchanges of water between the Gialova lagoon and the freshwater systems upstream and the sea downstream during the measurement period. Moreover, they provide estimates of salt mass fluxes associated with the saline water exchanges.

### 2.2.5 Simulation scenarios

To assess the effects of changing climatic conditions and water resource management on salinity in the Gialova lagoon, we use Eqs. (5) and (6) in a forward mode – that is, to estimate salinity variations through time based on hydrologic

fluxes. First, Eq. (5) is solved in discretized form to obtain  $Q_{\text{salt}}$  for given  $P$ ,  $E$ ,  $\Delta h/\Delta t$ , and  $Q_{\text{fresh}}$ ; second,  $Q_{\text{salt}}$  is inserted in Eq. (6), which is also solved in discretized form to calculate salinity  $C_G$ . The first step requires estimates of all hydrologic fluxes and the change in water storage except the unknown  $Q_{\text{salt}}$ . Measured precipitation and evaporation rates are modified to account for climatic changes, while the change in storage ( $dh/dt$ ) is maintained from current conditions given the strong coupling of water levels in the lagoon and in the sea (Sects. S1 and Fig. S1 in the Supplement). Sea level rise is not considered in these scenarios. The  $Q_{\text{fresh}}$  obtained under current conditions as described in Sect. 2.2.4 is modified to account for both climatic and water management changes. With these assumed  $P$ ,  $E$ ,  $Q_{\text{fresh}}$  and  $dh/dt$  values,  $Q_{\text{salt}}$  is calculated at each time step from the water balance (Eq. 5), and salinity is then readily obtained with the salt mass balance (Eq. 6).

We considered three climate change scenarios (Table 2): (C1) reduced precipitation, (C2) increased temperature (and thus evaporation), and (C3) combined reduction in precipitation and increase in temperature. All scenarios are based on results of a regional climate model forced by global climatic conditions under high CO<sub>2</sub> emissions (denoted as A2), with predictions extending to the year 2100 (Gao and Giorgi, 2008). For C1, a precipitation reduction up to 30 % was considered (while keeping current  $E$ ); for C2, evaporation was increased up to 20 % due to a mean annual temperature increase of 4 °C (while keeping current  $P$ ); for C3, the changes in  $P$  and  $E$  were compounded. Moreover, to assess the effects of changes in water–atmosphere exchanges in isolation, the lateral freshwater fluxes were either maintained as under current conditions or decreased to represent reductions in runoff for drier conditions driven by climate change.

In the simulations where lateral freshwater fluxes are decreased, a reduction coefficient was applied to all daily values of freshwater exchanges (water entering and leaving the lagoon). The reduction coefficients for each climate scenario were obtained by estimating future runoff  $R$  from catchments surrounding the lagoon using Budyko’s approach (Choudhury, 1999). First, the relation between long-term actual evapotranspiration (AET) and potential evapotranspiration (PET) was parameterized following Choudhury (1999). Second, long-term runoff was calculated as  $R = P - \text{AET}$  under the assumption of negligible change in water storage in the catchment,

$$R = P - \text{AET} = P - \frac{PPET}{(P^n + PET^n)^{\frac{1}{n}}}, \quad (12)$$

where  $n = 1.8$  (Choudhury, 1999). Assuming  $\text{PET} \approx E$ , Eq. (12) allows  $R$  to be estimated when  $P$  and PET change according to the climate scenarios C1–C3. Finally, reduction coefficients for the freshwater exchanges are calculated as the ratios of  $R$  under future conditions (from Eq. 12) over  $R$  under current conditions (i.e.,  $R = 167 \text{ mm yr}^{-1}$  for

$P = 695 \text{ mm yr}^{-1}$  and  $\text{PET} = 889 \text{ mm yr}^{-1}$ ; see Sect. 2.1). The obtained reduction coefficients are reported in Table 2.

These climatic scenarios were further combined with altered water resource management scenarios, in which we assumed that the lateral freshwater fluxes are either reduced due to intensified water use or increased by attempts to restore the Gialova lagoon to its original state of a brackish wetland (Table 2). To consider a wide range of possible management outcomes, we considered freshwater flux changes varying continuously from a 50 % reduction to a 50 % increase with respect to the current conditions, as estimated in Sect. 2.2.4. Management scenarios were implemented by varying the daily modeled values of  $Q_{\text{fresh}}$ , independently of climatic conditions (e.g., assuming that freshwater exchanges are fully controlled and not limited by water availability). As was also done for the climate change scenarios, all daily values of  $Q_{\text{fresh}}$  were varied, including freshwater losses from the lagoon, thereby imposing a control on the two-way connectivity of the lagoon with the surrounding freshwater bodies.

## 2.3 Measurements

### 2.3.1 Permanent equipment

Meteorological measurements were conducted with a Decagon Devices, Inc. system, including a relative humidity and air temperature sensor (VP4), a 2-D sonic anemometer (DS-2), a solar radiation sensor (pyranometer), and a rain gauge (ECRN-100), all installed in March 2016. Data were recorded using EM-50 loggers. These pieces of equipment, except for the anemometer, were located on the southern shore of the lagoon; the anemometer was installed on a concrete pillar in the middle of the lagoon (approximately 1 km from the other sensors) to minimize interference from vegetation and the nearby terrain. Three water quality and depth measurement points were set up in the lagoon – one at the southern shore next to the meteorological station, one next to the concrete pillar, and one on a PVC pole located near the northern shore (Fig. 1a). The southern and northern measurement sites were equipped with one conductivity–temperature–depth probe, while the central site had two probes at different depths (all CTD-10). For this study, salinity was estimated from the average value of the two central sensors, considered as representative for the whole lagoon (Sect. S2; Fig. S2). Missing data from late 2017 and January 2018 were gap-filled using the time series from the northern measurement site, which is well-correlated with that from the central measurement site (Fig. S3). Water depth variations were obtained from the northern sensor, which had no missing values and had remained at the same vertical position throughout the duration of the monitoring. The CTD-10 at the southern shore was not used as it exhibited significant tidal fluctuations in salinity due to the nearby channel

**Table 2.** Climatic and management scenarios. Variations are indicated as percentage change compared to current conditions. In scenarios C1–C3, freshwater inputs are either kept as under current conditions or decreased as a consequence of a higher potential evapotranspiration / precipitation ratio (black and red curves in Figs. 6a and 7a, respectively).

Scenario	Code	Explanation	Change in precipitation $P$ (% of current)	Change in evaporation rate $E$ (% of current)	Change in freshwater input $Q_{\text{fresh}}$ (% of current)	Source for $P$ and $E$ variations
Climate (Fig. 6)	C0	Current conditions	0 %	0 %	0 %	Fig. 4
	C1	Reduced $P$	0 % to –30 %	0 %	0 % to –57 %	Gao and Giorgi (2008)
	C2	Increased $E$	0 %	0 % to +20 %	0 % to –21 %	Gao and Giorgi (2008)
	C3	Reduced $P$ , increased $E$	0 % to –30 %	0 % to +20 %	0 % to –67 %	Gao and Giorgi (2008)
Management and climate (Fig. 7)	Decreased or increased $Q_{\text{fresh}}$	All climatic scenarios C0–C3	All climatic scenarios C0–C3	–50 % to +50 % (independent of $P$ and $E$ )	Fig. 4 and Gao and Giorgi (2008)	

connecting the Gialova lagoon and Navarino Bay and thus cannot be regarded as representative for the whole lagoon.

### 2.3.2 Field campaigns and areal estimates of salinity

The representativeness of the salinity measurements from the central site was tested by comparing the point measurements to distributed measurements collected along the shore and in the lagoon during several intensive campaigns from 1995 to 2018 (Sect. S2). The campaigns were conducted at different times of the year to span the full range of salinities occurring in the lagoon. Distributed data from these campaigns were used to estimate areal average salinities that were compared to the point measurements described in Sect. 2.3.1. The comparison yielded a linear relation close to the 1 : 1 line ( $R^2 = 0.95$ ) that was used to scale up the point measurements to the whole lagoon area (Fig. S2). A summary of the areal salinity estimates from all the measurement campaigns is also shown in Fig. S4 as a function of month to illustrate its seasonal cycle.

### 2.3.3 Data processing

Meteorological data were collected with a sampling interval of 5 min and averaged (or accumulated for rainfall and solar radiation) over a day. Gaps in the meteorological data record were filled using time series from two other meteorological stations – one located in an olive orchard 5 km from the Gialova lagoon, the other located at Methoni (National Observatory of Athens, 2019). Details on the gap-filling procedure are reported in the Sect. S3.

Water electrical conductivity measurements included erroneous readings (downward peaks with unreasonably low conductivity values with respect to a well-defined upper envelope). These erroneous values were removed with a two-step de-spiking algorithm before daily averaging. The al-

gorithm first detected and removed outliers (values lower than the 10th percentile) in a moving window of 4 h. Second, data points that caused the standard deviation in the moving window to be higher than 4 times the standard deviation in a window without any error were also removed. Conductivity values (expressed in  $\text{mS cm}^{-1}$ ) were converted to salt concentrations ( $\text{g L}^{-1}$ ) using the empirical relation,  $C_G = 0.4665\text{EC}^{1.0878}$ , where EC is the electrical conductivity at 25 °C (Williams, 1986) (temperature corrections were performed when logging the data).

Salinity in the Ionian Sea is set to a constant value of  $38.5 \text{ g L}^{-1}$ . This value was obtained using monthly data from 1 m depth for the period 2008–2012 from the measurement buoy number 68 422 (Pylos) of the European Marine Observation and Data Network (French Research Institute for Exploitation of the Sea, 2018). The buoy was located approximately 10 km southwest of the Gialova lagoon and is assumed representative of the salinity in both Navarino and Voidokilia bays. Seasonal variations in salinity were minor ( $38.2$  to  $38.9 \text{ g L}^{-1}$ ) compared to the variability of salinity in the Gialova lagoon, thereby supporting our assumption of time-invariant sea water salinity.

## 3 Results

### 3.1 Water fluxes under current conditions

The study period is characterized by typical Mediterranean conditions, with mild and wet winters, and warm and dry summers (Figs. 2 and 3). Even though winters receive most of the rainfall, some late summer storms were exceptionally intense (140 mm between DOY 250 and 251 of 2016). This precipitation regime, together with intense summer evaporation rates sustained by high solar radiation and temperature (Fig. 3d), contributes to strong seasonal variations in salin-

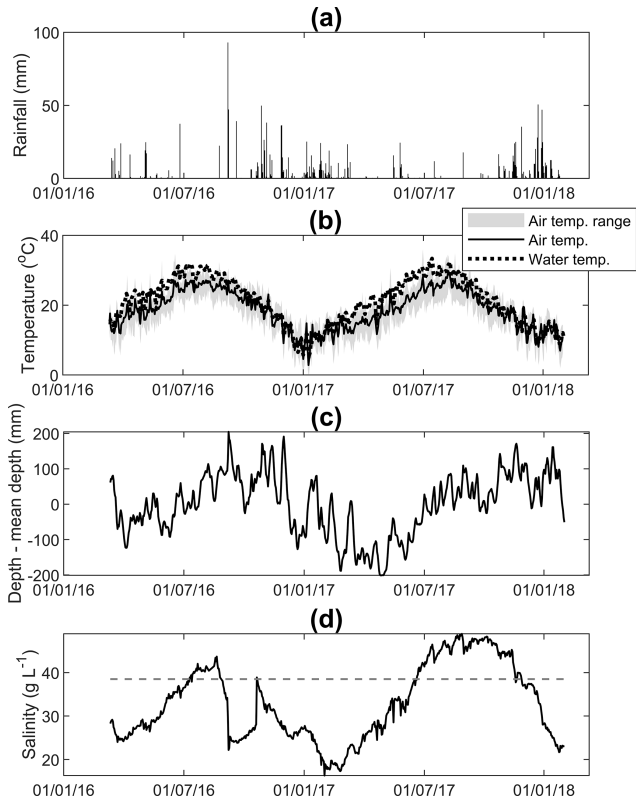


**Figure 2.** Time series of (a) daily total precipitation, (b) daily mean air and lagoon water temperatures (solid and dashed curves, respectively), daily air temperature range (shaded area), (c) lagoon water depth (normalized by the mean depth), and (d) salinity.

ity (Fig. 2d). Salinity tends to increase during the spring and throughout the summer, peaking in late summer or early fall (hypersaline conditions, defined here with respect to the average seawater salinity of 38.5 g L<sup>-1</sup>). Fall and winter freshwater inputs eventually restore salinity below values typical of the Ionian Sea. These seasonal fluctuations are consistent with those reported in earlier studies (summarized in Fig. S4) and depend on both hydroclimatic conditions (both intra- and interannual fluctuations in water balance) and interannual changes in water management (Sect. 4.3).

The seasonal pattern of salinity is punctuated by sudden events in response to intense rainfall events. The most notable event occurred on DOY 251 of 2016, leading to a rapid decrease in salinity from 35 to 22 g L<sup>-1</sup>, with the lower level sustained over the following month and a half. High salinity is associated with high water levels (Fig. 2c), which tend to occur during the warmer months despite their higher evaporation rate. Water levels vary largely as a function of tidal fluctuations in the Ionian Sea (Sect. S1) and are weakly correlated to individual rainfall events or the seasonal fluctuations in hydroclimatic variables. Specifically, the water levels in the Gialova lagoon lag approximately one day behind

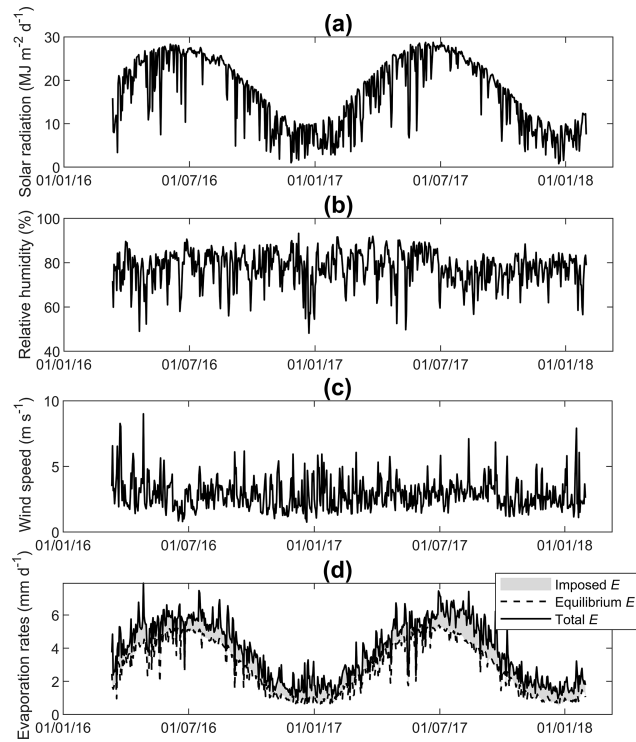


**Figure 3.** Time series of (a) daily total incoming shortwave radiation, (b) daily mean relative humidity, (c) wind speed, and (d) calculated evaporation rates (Eq. 7), further decomposed into equilibrium evaporation (dashed black curve) and “imposed E”; i.e., the aerodynamic component of evaporation (shaded area).

those of the Ionian Sea (the Pearson correlation coefficient is maximized with a lag of one day,  $r = 0.78$ ; Fig. S1).

Figure 4a illustrates monthly averaged hydrologic fluxes, including precipitation, evaporation and changes in water depth in the lagoon. Evaporation is generally higher than precipitation, as expected in Mediterranean climates (Fig. 1). Variations in storage (i.e., water depth) are more dynamic than in the other two lagoon–atmosphere fluxes and do not compensate for the negative hydrologic balance of the lagoon. Given the necessity of water balance closure over the lagoon, this suggests that other water exchanges via groundwater and surface water play a significant role. The coupled water and salt mass balances (Eqs. 10 and 11) facilitate estimation of the freshwater and saline water exchanges between the Gialova lagoon and surrounding water bodies (Fig. 4b), through closure of the lagoon hydrologic balance. The estimated fluxes are on the same order of magnitude of rainfall and evaporation rates, reaching monthly averages of  $\pm 10 \text{ mm d}^{-1}$ , and highly variable. Freshwater exchanges are generally positive, indicating inputs to the lagoon, as might be expected by the presence of a freshwater aquifer, as well as diffuse and point inputs from streams and springs feeding the main water body of the lagoon. However, during the sudden salinity increase on DOY 294 of 2016, the model sug-



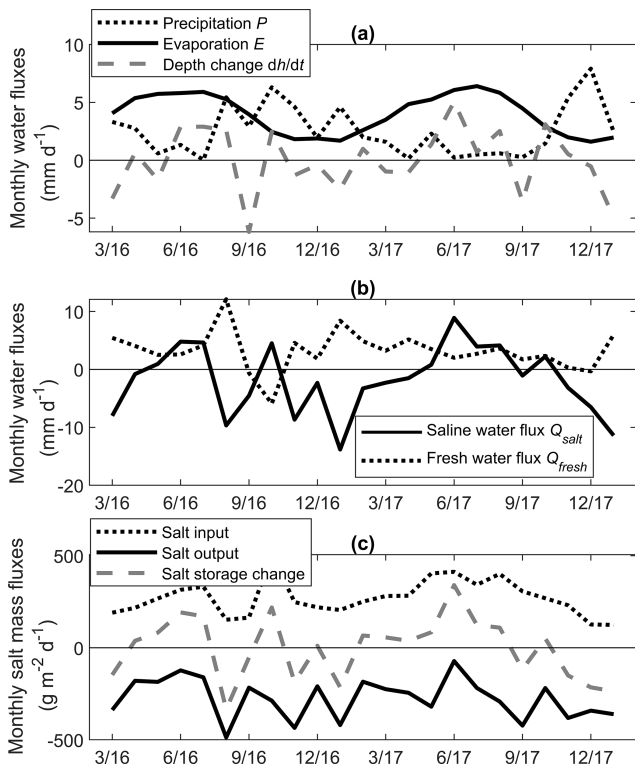


**Figure 4.** (a) Mean monthly hydrologic fluxes, (b) saline and fresh water exchange fluxes (from Eqs. 10 and 11, respectively), and (c) salt mass fluxes. Positive (negative) fluxes indicate water inputs (outputs from) the Gialova lagoon.

gests a rapid outflow of freshwater (where outflow is a negative flux). This outflow is consistent with the constraint set by the salt water balance and is needed to explain the measured increase in salt concentration at nearly constant water level. Throughout the study period, the saline fluxes often change sign, indicating alternate periods during which either water from the Ionian Sea enters the lagoon (positive sign, generally during the summer months), or water from the lagoon flows into the sea (negative sign, generally during winter and spring).

Some of the daily fluxes shown in Figs. 2 and 3 and the calculated saline and fresh water exchange fluxes are correlated (Table 3). Precipitation and evaporation rates are negatively correlated due to their seasonal cycle (Figs. 2a and 3d), and variations in water level are positively correlated to precipitation rates. These correlations emerge from intrinsic processes and relations among hydrologic variables that are not explicitly parameterized in the present water and mass balance equations, whereas other correlations are expected from the physical balance relations expressed mathematically in Eqs. (10) and (11). In particular, saline water fluxes are (strongly) positively correlated with water level variations and (strongly) negatively correlated with freshwater fluxes, as implied by Eq. (11). The occurrence of the strong cor-

**Table 3.** Pearson correlation coefficients between pairs of hydrologic fluxes (or change in storage), as calculated with Eqs. (10) and (11) at the daily timescale (asterisks (\*) indicate significant correlations,  $p < 0.001$ ).

	$dh/dt$	$P$	$E$	$Q_{\text{fresh}}$	$Q_{\text{salt}}$
$dh/dt$	1.00	0.29*	0.00	0.05	0.63*
$P$		1.00	-0.29*	-0.14*	-0.05
$E$			1.00	0.05	0.15*
$Q_{\text{fresh}}$				1.00	-0.66*
$Q_{\text{salt}}$					1.00

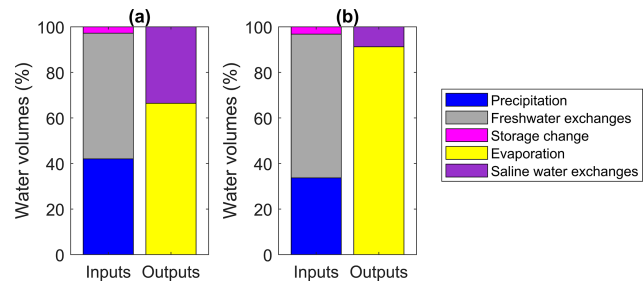


**Figure 5.** Water budgets over the whole study period for (a) current conditions and (b) future conditions (scenario C3: reduced precipitation and increased evaporation rate; see Table 2). Water volumes are expressed as a percentage of the total volume entering or leaving the lagoon, and only the net saline water exchanges are included in the budgets.

relation between fresh and saline water fluxes indicates that variability in water exchanges between the lagoon and the sea or land dominates over variability imposed by water-atmosphere exchanges.

When considering the entire study period, precipitation represents  $\approx 40\%$  of the water inputs to the lagoon, whereas the remaining  $60\%$  is driven by freshwater exchanges, with a minor contribution by change in water level (Fig. 5a, left bar). Evaporation represents  $\approx 70\%$  of the water outputs from the lagoon, and the remaining  $30\%$  is caused by saline water loss from the lagoon to the Ionian Sea (Fig. 5a, right bar).

### 3.2 Water fluxes under changed climate and water management

Climatic changes reducing precipitation and increasing evaporation rate (scenario C3) are expected to alter the water balance with respect to current conditions (Fig. 5b). The overall lower inputs and higher evaporative losses are compensated by lower outputs of saline water from the lagoon. Note that in Fig. 5b we assumed that freshwater inputs remained as they are today, but without any management effort, the flows from the surface freshwater bodies would most likely decrease as a result of lower precipitation and higher evapotranspiration in the catchments feeding the lagoon (Sect. 4.3). Figure 6a

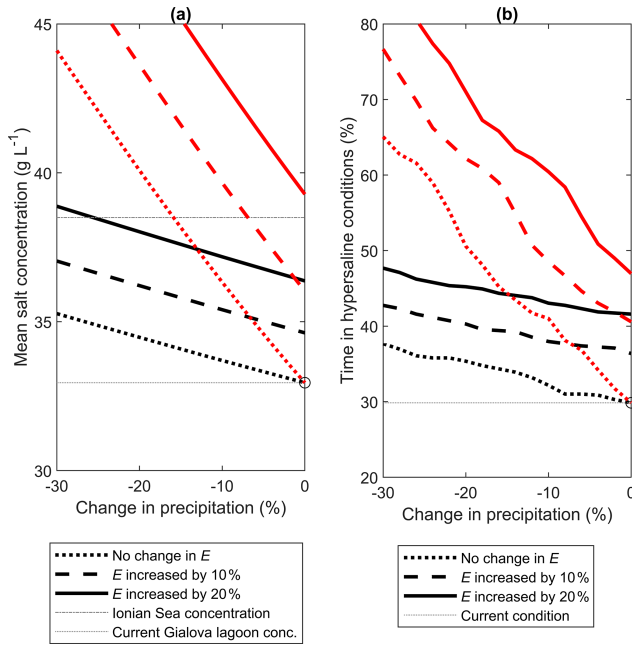


**Figure 6.** Effect of climatic changes on (a) the mean salt concentration in the Gialova lagoon and (b) the percentage of time under hypersaline conditions. Different line styles refer to three scenarios for changes in evaporation rate; red lines refer to scenarios where freshwater fluxes are reduced as a result of climatic changes. Percentage time is calculated for the two simulation years; for visual reference, the grey horizontal dotted lines indicate current salinity and duration of hypersaline conditions in the Gialova lagoon, and the grey dotted–dashed line in (a) indicates salt concentration in the Ionian Sea as of today; current conditions are indicated by open circles.

shows predicted changes in the mean salinity of the Gialova lagoon as a function of gradual precipitation reduction on the abscissa, in combination with unchanged (scenario C1) or increased evaporation rate (C3) while keeping current freshwater inputs (black lines). In addition, the effect of reduced freshwater inputs due to lower runoff from the surrounding catchments is considered (red lines). An increase of 10 % in evaporation rate alone (as would be caused by higher temperatures) is predicted to increase salinity by approximately 5 %. Any decrease in precipitation in combination with an increasing evaporation rate further increases salinity due to the accumulation of salt from the marine sources. Salt accumulates because it enters the lagoon during increases in sea water level, but it does not leave it again under decreases in sea level due to saline outflows (Fig. 5b). However, for a given evaporation rate, when both precipitation and freshwater inputs are decreased, salinity increases more than when only precipitation is decreased (compare red and black lines).

The time spent under hypersaline conditions is a more useful ecological indicator than mean salt concentration, as it directly impacts the ecological actors. Figure 6b shows how the percentage of time under hypersaline conditions varies

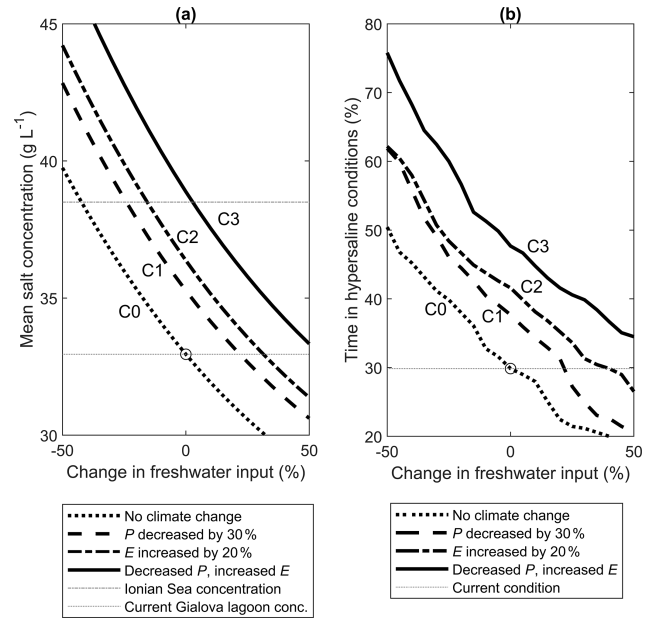


**Figure 7.** Effect of changes in freshwater input on (a) the mean salt concentration in the Gialova lagoon and (b) the percentage of time under hypersaline conditions, under different climatic scenarios (different line styles; see details in Table 2). Percentage time is calculated for the two simulation years; for visual reference, the grey horizontal dotted lines indicate current salinity and duration of hypersaline conditions in the Gialova lagoon, and the grey dotted–dashed line in (a) indicates salt concentration in the Ionian Sea as of today; current conditions are indicated by open circles.

with hydroclimatic changes (similar to those in Fig. 6a). Decreasing precipitation alone moderately increases the time in hypersaline conditions from the current 3 months per year. As noted for changes in salinity (Fig. 6a), higher evaporation rates – especially when compounded with lower freshwater inputs – yield longer periods under hypersaline conditions, potentially up to most of the year in the worst-case scenario.

Altering the management of surface freshwater also affects salinity in the Gialova lagoon, as shown in Fig. 7a. Allowing more (less) freshwater to flow into the lagoon leads to a decrease (increase) in salinity under any climate scenario. The change in salinity is nonlinearly related to changes in freshwater input, consistent with an overall salt dilution effect. Under current climatic conditions (dotted line in Fig. 7a), a 50 % reduction in freshwater inflows leads to an annual mean salinity similar to that of the Ionian Sea. Under future climatic conditions, a similar decrease in freshwater inputs increases salinity in the lagoon to values that are much higher than in the Ionian Sea. To prevent a transition to a saline lagoon under future climatic conditions, freshwater inputs need to be increased by  $\approx 25\%$ ,  $30\%$  or more than  $50\%$  under the three scenarios of increased aridity (C1, C2, and C3, respectively). These percentages can be seen in Fig. 7a at the intersections between the current salt concentration (horizontal

grey dotted line) and the three curves representing salt concentrations under the three climate scenarios.

Similar patterns emerge in Fig. 7b for the duration of hypersaline conditions. With lower freshwater inputs combined with climatic changes, the model predicts hypersaline conditions for up to 9 months per year. Only increasing freshwater inputs, in the absence of climatic changes, limits hypersaline conditions to about 2.5 months per year.

## 4 Discussion

### 4.1 Approach limitations

The proposed approach rests on several assumptions that may affect our results and conclusions. First, this is a lumped approach that neglects spatial variability by assuming well-mixed conditions vertically and laterally. This lumped approach is comparable in scope to previous efforts on lakes and lagoons where no distributed salinity data are available (Assouline, 1993; Martinez-Alvarez et al., 2011; Obrado et al., 2008; Rodellas et al., 2018). Following the well-mixed assumption, the salinity in the central measurement point (averaging measurements of two probes spaced 25 cm apart vertically) is regarded as representative of average salinity over the whole lagoon. While this might not be always the case, especially after strong rain events causing high localized freshwater inputs from the sluice gate connecting the Tyflomitis diversion canal to the lagoon (Maneas et al., 2019), we have shown that temporal variability in spatial average salinity is well captured by the point measurements (Fig. S2). Moreover, vertical mixing is ensured by wave motion and tidal fluctuations in this shallow water body. Thermal stratification is minimal at the temporal scale of this study, as indicated by highly correlated water temperatures at the two sampled depths in the central measurement point (Pearson correlation coefficient  $r = 0.998$ ). However, salt fluxes depend on salinity levels where hydrological flows occur. Thus, a lumped approach has the potential to overestimate salt fluxes by over-emphasizing salinity gradients. Assessing the consequences of this assumption requires a detailed hydrodynamic model of the lagoon.

The water balance Eq. (1) constrains the unknown freshwater inputs, implying that any uncertainty in the other water fluxes affects the freshwater input results. For example, a sudden increase in salinity not associated with significant water level change leads to both saline water inputs into and freshwater losses from the lagoon, in order to close both the salt and the water balance. The freshwater losses are difficult to interpret, but could be explained as a loss of relatively fresh water far from the lagoon–sea canal, which is substituted by more saline water from the Ionian Sea. It would be valuable to monitor two-way water exchanges at the sluice gates by regulating water exchanges from inland water bodies to test this model implication. In the long term, however,

freshwater inputs dominate the water balance, as expected under a Mediterranean climate with relatively low precipitation.

Moreover, for our well-mixed assumption to hold, the water and salt balances used cannot be resolved at timescales shorter than the equilibration time for the lagoon, which we estimate to be on the order of one day (Fig. S1). Therefore, significant exchanges of water and salt occurring due to shorter-term fluctuations in sea water level are neglected but could be important at longer timescales. To address the limitations of the well-mixed assumption and gain insights into water exchanges at subdaily timescales, the Gialova lagoon should be represented by a spatially explicit hydrodynamic model; such models have been developed and used in other recent studies for the simulation of coastal and semi-enclosed sea conditions at various scales and under different hydroclimatic and/or water management scenarios (Chen et al., 2019; Vigouroux et al., 2019).

Another source of uncertainty may be introduced by attributing changes in electrical conductivity solely to salinity changes (Williams, 1986). Other solutes can impact electrical conductivity but not salinity, potentially leading to errors. For the current application, where we focus on relatively short time periods, there are likely minimal land cover or nutrient load changes, which limits the variability of electrical conductivity due to other constituents. Also, assuming relatively stable flow pathway distributions in the landscape over the study period, the geochemical signature of groundwater is likely constant enough so that the main driver of changes in electrical conductivity is salinity from sea water rather than terrestrial sources.

### 4.2 The hydrologic balance of the Gialova lagoon under current and future climate

In the absence of direct flow measurements, the water balance approach presented provides estimates of the major hydrologic fluxes exchanged through the Gialova lagoon (Fig. 4), allowing its overall water balance over the 2-year study period to be assessed. This water balance, expressed in terms of relative water partitioning among different input and output fluxes (Fig. 5), can be compared to hydrologic flux estimates in other Mediterranean lagoons. Mar Menor – a much larger lagoon in southern Spain, connected to the Mediterranean sea via five channels (Martinez-Alvarez et al., 2011) – receives water mostly from marine sources (62 %), with smaller contributions from precipitation (24 %) and runoff (15 %; Martinez-Alvarez et al., 2011). In contrast – and similar to the Gialova lagoon – water inputs to the small Albufera des Grau (Menorca, Spain) are dominated by runoff (71 %), followed by precipitation (29 %), while in the long term this lagoon has a net outflow to the sea (Obrador et al., 2008). Albufera des Grau loses more water through evaporation than the Gialova lagoon (76 % vs. 60 %), and correspondingly less through net exchanges with the sea (24 % vs. 40 %). Despite

these differences, our estimates based on mass balance calculations are still reasonable when compared to similar lagoons in the Mediterranean basin.

These estimates based on net water exchanges between the lagoons and the sea mask the underlying patterns of gross water exchanges. We estimate large two-way exchanges with the Ionian Sea, facilitated by the canal that connects the lagoon with Navarino Bay (minimum cross section of  $7 \text{ m}^2$ ). Saline water inflows amount to  $2490 \text{ mm yr}^{-1}$  and outflows to  $3200 \text{ mm yr}^{-1}$ , with a net loss of water from the lagoon to the sea of  $710 \text{ mm yr}^{-1}$  (with all flows normalized by the average surface area of the lagoon). These gross water fluxes are on the same order of magnitude as those exchanged by Mar Menor (gross saline water input:  $5600 \text{ mm yr}^{-1}$ ; gross output to the sea:  $4800 \text{ mm yr}^{-1}$ ; Martinez-Alvarez et al., 2011) but are larger than those exchanged by Albufera des Grau (gross saline water input:  $200 \text{ mm yr}^{-1}$ ; gross output to the sea:  $900 \text{ mm yr}^{-1}$ ; Obrador et al., 2008). This is not surprising, because the latter is connected to the sea via a narrow channel regulated by a floodgate, which limits the water exchanges, compared to the large channels connecting Mar Menor to the sea.

The seasonal pattern characterized by freshwater inputs in the winter and spring and saline water inputs primarily in the summer and autumn is similar to that observed in other Mediterranean lagoons (Obrador et al., 2008; Stump et al., 2014). The estimated freshwater inputs amount to  $1170 \text{ mm yr}^{-1}$ , which are mainly partitioned between evaporation ( $\approx 40\%$ ) and water losses to the Ionian Sea ( $\approx 60\%$ ). Currently, the main freshwater input to the lagoon is from Tyflomitis stream and artesian springs. In that area east of the lagoon, hydraulic gradients are steeper, allowing freshwater aquifers to deliver water to the Tyflomitis springs (Pantazis, 2019). Flow estimates for these water sources are uncertain and currently range between  $0.5 \times 10^6$  and  $2.0 \times 10^6 \text{ m}^3 \text{ yr}^{-1}$  (Maneas et al., 2019), equivalent to approximately 220 to  $890 \text{ mm yr}^{-1}$  of freshwater inputs after normalizing the flow rates by the lagoon area. Our estimated freshwater inputs are higher but still reasonable, considering that part of the water from Tyflomitis is diverted to Navarino Bay, but that unquantified groundwater flows likely contribute freshwater to the lagoon as well.

The Mediterranean region is projected to become warmer and drier (Cheval et al., 2017; Gao and Giorgi, 2008). By reducing precipitation and associated runoff, and increasing evaporation rates, future climatic conditions are expected to increase salinity unless freshwater inputs now diverted from around the lagoon to the Ionian Sea are restored. To assess the consequences of these climatic changes, we first calculated how salinity responds to independent variations in precipitation, evaporation, and freshwater inputs (black curves in Fig. 6). Results show – as expected – increases in salt concentrations for all these hydrologic changes. Similarly, the time spent under hypersaline conditions is expected to increase with such climatic changes and without intervention

measures (black curves in Fig. 7). It is reasonable to expect that the freshwater inputs will be reduced due to not only lower runoff from surrounding catchments under more arid conditions (Eq. 12), but also increased water abstractions (Sect. 4.3). Using the Budyko curve to estimate changes in runoff from the catchments feeding the Gialova lagoon (Eq. 12), we found that a reduction in precipitation, an increase in PET, and both changes together (as in Table 2), respectively cause runoff and thus freshwater inputs to decrease by 57 %, 21 %, and 67 % from the current level. Concurrently, groundwater levels are also expected to decrease, potentially causing saline intrusions around the lagoon – a process already ongoing at least at the end of the dry season (Pantazis, 2019). The expected reductions in freshwater inputs will likely worsen the lagoon conditions, increasing salinity during winter and spring more than predicted when climate does not constrain freshwater inputs.

We have not assessed the effects of long-term changes in sea level. The water levels in the Gialova lagoon are well-coupled to those in the Ionian Sea, with a time lag of one day (Fig. S1). As a result of this tight connection, sea level rise is expected to be mirrored by a rise in lagoon water level. This may alter the exchanges of saline water with Navarino Bay, since the low Divari sand barrier may be eroded, creating more channels that link the lagoon to the sea. Faster exchanges with Navarino Bay imply that hypersaline conditions during the summer may be avoided, but also that the duration of periods with brackish water would then be shortened. Resolving this question is beyond the scope of this study, but can be addressed in future studies coupling projections of sea level rise to possible geomorphological changes in the area.

### 4.3 Management options for salinity regulation

Water and land in the Peloponnese peninsula, where the Gialova lagoon is situated (Fig. 1a), have been intensively used at least for the last 6000 years, often resulting in major changes in hydrologic functioning (Butzer, 2005; Weiberg et al., 2016). Land conversion to agriculture during periods of population growth and back to natural vegetation when pressure decreased, resulted in periods of sustained erosion, change in soil surface properties, altered evapotranspiration rates associated with varying vegetation types, and modifications of surface flow pathways due to construction of terraces and other water-conserving systems. These alterations have likely caused variable freshwater inputs to coastal lagoons, which have been compounded with long-term hydroclimatic trends and geomorphological processes (Emmanouilidis et al., 2018). Arguably, the most intense alterations occurred after 1960, when the streams feeding the lagoon were diverted, and the lagoon was drained and isolated from the sea to expand agricultural areas (Maneas et al., 2019). Since 1976, however, hydrologic linkages with the sea and partly with the surface freshwater sources have been restored. In 1999,

sluice gates were also opened to connect the drainage canals to the lagoon. Despite these restoration efforts, today the Gialova lagoon remains poorly connected with freshwater sources and is thus more saline than before the drainage (Figs. 2 and S4). Earlier measurements support this view: the opening of the sluice gates increased surface hydrological connectivity and allowed salinity to decrease from summer values above  $60 \text{ g L}^{-1}$  to between 30 and  $50 \text{ g L}^{-1}$  (compare data from the 1995–1996 field campaign to those of the later campaigns in Fig. S4).

As also shown in previous studies (Arvanitidis et al., 1999; Koutsoubas et al., 2000; Obrador et al., 2008), salinity varies seasonally, with higher values during the dry period (June–October) and lower values during the wet period (November–March) (Fig. S4). However, in contrast to these studies our findings indicate that water conditions should be characterized as saline or even hypersaline during the months June–November, with more brackish conditions occurring only during the wetter winter and spring seasons. High salinity has been highlighted in previous studies on the Gialova lagoon as one of the main factors leading to dystrophic crisis events and fish mortality (Arvanitidis et al., 1999; Koutsoubas et al., 2000), similar to other Mediterranean lagoons experiencing dystrophic crises after prolonged drought (Obrador et al., 2008). The combined effects of increased salinity and limitation in water circulation has led to extensive reed and cattail mortality, thereby deteriorating important habitats for water birds (Maneas et al., 2019). On the one hand, the lagoon has an important fishery value (Koutsoubas et al., 2000), and the opening of additional canals with the Navarino Bay has been suggested as a way to improve water circulation and fishing (Arvanitidis et al., 1999). On the other hand, the lagoon is part of a wider protected bird area. Increased freshwater inputs could be favorable for bird conservation, but could also negatively affect the fishing in the lagoon if these inputs are of low quality due to agricultural contaminants. A sustainable future water management strategy should aim to create favorable conditions for both fishing and bird conservation. Such a strategy will need to be based on more data, from not only systematic monitoring of fish stocks, bird status and water parameters such as oxygen levels and nutrients concentrations, but also from knowledge from the local fishing community.

In the current context of water scarcity and competing water demands in the Mediterranean region – and Greece in particular (Destouni and Prieto, 2018; Klein et al., 2015; Perez-Ruzafa et al., 2011) – managing freshwater inputs to the Gialova lagoon can be challenging. Our results show that, to adapt to expected climatic conditions by the end of 2100 and maintain the current annual average salinity in the lagoon, a more than 50 % increase in freshwater inputs should be achieved, corresponding to at least  $1750 \text{ mm yr}^{-1}$  (Fig. 6b). To assess if such a 50 % increase is feasible, the total water resources currently available must be quantified. Combining the flow rates of the two streams that before being

diverted reached and fed the lagoon (Maneas et al., 2019), the total surface water that would be naturally available is between 2400 and  $3100 \text{ mm yr}^{-1}$  (values are normalized by lagoon area and include the contributions from Tyflomitis springs reported in Sect. 4.2), which in principle could fulfill the demand to stabilize salinity. These estimates are higher than, but considering the uncertainties still comparable with the  $2200 \text{ mm yr}^{-1}$  obtained from the Budyko curve (Eq. 12). These estimates do not reflect the expected reduction in precipitation and increased evaporation in the coming decades, which will decrease both runoff to and groundwater flow in the lagoon. In the worst-case climate scenario of 67 % lower runoff (Sect. 4.2), the available surface water inflow could be limited to the range  $810\text{--}1030 \text{ mm yr}^{-1}$  – clearly not enough to increase the current estimated freshwater inputs. This estimate is conservative; if water abstraction increases as might be required to maintain agricultural productivity in the catchment (Maneas et al., 2019), freshwater inputs would be even lower. Thus, under future conditions, managing freshwater inputs to maintain current salinity levels appears unlikely.

## 5 Conclusions

We have shown through a mass balance approach that under current climatic conditions the Gialova lagoon receives about 40 % of water inputs from precipitation and 60 % from surface and groundwater freshwater sources. Under these conditions, the lagoon is hypersaline for nearly 30 % of the year. Under future drier and warmer conditions, the water balance is predicted to change towards higher evaporation losses, associated with higher salinity levels and in the worst-case scenario prevalence of hypersaline conditions. The same modeling approach suggests that managing the freshwater inputs available today could reduce salinity. However, under future conditions such efforts might not be enough to stabilize salinity to current levels because runoff will likely be reduced by climatic factors and possibly higher water abstractions.

*Data availability.* The primary dataset (meteorological and water quality parameters; calculated evaporation rates) is archived in the open-access database of the Bolin Centre for Climate Research (<https://doi.org/10.17043/manzoni-2020>, Manzoni et al., 2020).

*Supplement.* The supplement related to this article is available online at: <https://doi.org/10.5194/hess-24-1-2020-supplement>.

*Author contributions.* SM and SWL developed the mathematical model with feedback from GD. SM and GM collected and analyzed the 2016–2018 data. GM collected and analyzed the historical data. AS conducted the spatial analysis in Sect. S2. BEP provided and analyzed meteorological data from the NOAA/IERSD station at

Methoni. SM drafted the paper. All authors discussed the content, provided feedback and wrote the final paper.

*Competing interests.* The authors declare that they have no conflict of interest.

*Acknowledgements.* We thank Agnes Classon and Kim Lundmark for assistance installing the equipment and preliminary data analyses, Eirini Makopoulou and Christos Pantazis for preparing Fig. 1a, and two reviewers for their constructive criticism. This study has been conducted using sea water salinity data from EU Copernicus Marine Service Information, and sea water levels from the UNESCO Intergovernmental Oceanographic Commission.

*Financial support.* This research has been supported by the Navarino Environmental Observatory (NEO), the EU Horizon 2020 project COASTAL (H2020-RUR-02-2017, grant no. 773901 to Giorgos Maneas and Georgia Destouni), the Bolin Centre for Climate Research, and by the Swedish Research Councils (Vetenskapsrådet, Formas) and Sida (project VR 2016-06313 to Anna Scaini and Stefano Manzoni).

The article processing charges for this open-access publication were covered by Stockholm University.

*Review statement.* This paper was edited by Dimitri Solomatine and reviewed by two anonymous referees.

## References

- Allen, R. G., Pereira, L. S., Raes, D., and Smith, M.: Crop evapotranspiration – Guidelines for computing crop water requirements, FAO Irrigation and drainage paper 56, FAO – Food and Agriculture Organization of the United Nations, Rome, 1998.
- Arvanitidis, C., Koutsoubas, D., Dounas, C., and Eleftheriou, A.: Annelid fauna of a Mediterranean lagoon (Gialova lagoon, southwest Greece): community structure in a severely fluctuating environment, *J. Mar. Biol. Assoc. UK*, 79, 849–856, 1999.
- Assouline, S.: Estimation of lake hydrologic budget terms using the simultaneous solution of water, heat, and salt balances and a Kalman filtering approach – Application to Lake Kinneret, *Water Resour. Res.*, 29, 3041–3048, <https://doi.org/10.1029/93wr01181>, 1993.
- Assouline, S., Li, D., Tyler, S., Tanny, J., Cohen, S., Bou-Zeid, E., Parlange, M., and Katul, G. G.: On the variability of the Priestley–Taylor coefficient over water bodies, *Water Resour. Res.*, 52, 150–163, <https://doi.org/10.1002/2015wr017504>, 2016.
- Butzer, K. W.: Environmental history in the Mediterranean world: cross-disciplinary investigation of cause-and-effect for degradation and soil erosion, *J. Archaeolog. Sci.*, 32, 1773–1800, <https://doi.org/10.1016/j.jas.2005.06.001>, 2005.
- Chen, Y. Y., Vigouroux, G., Bring, A., Cvetkovic, V., and Destouni, G.: Dominant Hydro-Climatic Drivers of Water Temperature, Salinity, and Flow Variability for the Large-Scale System of the Baltic Coastal Wetlands, *Water*, 11, 552, <https://doi.org/10.3390/w11030552>, 2019.
- Cheval, S., Dumitrescu, A., and Birsan, M. V.: Variability of the aridity in the South-Eastern Europe over 1961–2050, *Catena*, 151, 74–86, <https://doi.org/10.1016/j.catena.2016.11.029>, 2017.
- Choudhury, B.: Evaluation of an empirical equation for annual evaporation using field observations and results from a biophysical model, *J. Hydrol.*, 216, 99–110, [https://doi.org/10.1016/S0022-1694\(98\)00293-5](https://doi.org/10.1016/S0022-1694(98)00293-5), 1999.
- Destouni, G. and Prieto, C.: Robust Assessment of Uncertain Freshwater Changes: The Case of Greece with Large Irrigation – and Climate-Driven Runoff Decrease, *Water*, 10, 1645, <https://doi.org/10.3390/w10111645>, 2018.
- Destouni, G., Asokan, S. M., and Jarsjo, J.: Inland hydro-climatic interaction: Effects of human water use on regional climate, *Geophys. Res. Lett.*, 37, L18402, <https://doi.org/10.1029/2010gl044153>, 2010.
- Dounas, K. and Koutsoubas, D.: Environmental Impact Study on pollution from petroleum products in Navarino Bay and Gialova Lagoon wetland, Institute of Marine Biology of Crete, Crete, 298 pp., 1996.
- Duan, Z. and Bastiaanssen, W. G. M.: Evaluation of three energy balance-based evaporation models for estimating monthly evaporation for five lakes using derived heat storage changes from a hysteresis model, *Environ. Res. Lett.*, 12, 024005, <https://doi.org/10.1088/1748-9326/aa568e>, 2017.
- Emmanouilidis, A., Katrantsiotis, C., Norstrom, E., Risberg, J., Kylander, M., Sheik, T. A., Iliopoulos, G., and Avramidis, P.: Middle to late Holocene palaeoenvironmental study of Gialova lagoon, SW Peloponnese, Greece, *Quatern. Int.*, 476, 46–62, <https://doi.org/10.1016/j.quaint.2018.03.005>, 2018.
- French Research Institute for Exploitation of the Sea: Oceanographic Data, available at: <http://en.data.ifremer.fr/pdmi/portalssearch/main>, last access: 27 November 2018.
- Gao, X. J. and Giorgi, F.: Increased aridity in the Mediterranean region under greenhouse gas forcing estimated from high resolution simulations with a regional climate model, *Global Planet. Change*, 62, 195–209, <https://doi.org/10.1016/j.gloplacha.2008.02.002>, 2008.
- Jaramillo, F., Licero, L., Åhlen, I., Manzoni, S., Rodríguez-Rodríguez, J. A., Guittard, A., Hylin, A., Bolaños, J., Jawitz, J., Wdowinski, S., Martínez, O., and Espinosa, L. F.: Effects of Hydroclimatic Change and Rehabilitation Activities on Salinity and Mangroves in the Ciénaga Grande de Santa Marta, Colombia, *Wetlands*, 38, 755–767, <https://doi.org/10.1007/s13157-018-1024-7>, 2018.
- Jarsjo, J. and Destouni, G.: Groundwater discharge into the Aral Sea after 1960, *J. Mar. Syst.*, 47, 109–120, <https://doi.org/10.1016/j.jmarsys.2003.12.013>, 2004.
- Klein, J., Ekstedt, K., Walter, M. T., and Lyon, S. W.: Modeling Potential Water Resource Impacts of Mediterranean Tourism in a Changing Climate, *Environ. Model. Assess.*, 20, 117–128, <https://doi.org/10.1007/s10666-014-9418-2>, 2015.
- Koutsoubas, D., Dounas, C., Arvanitidis, C., Kornilios, S., Petihakis, G., Triantafyllou, G., and Eleftheriou, A.: Macrobenthic community structure and disturbance assessment in Gialova lagoon, Ionian Sea, *ICES J. Mar. Sci.*, 57, 1472–1480, <https://doi.org/10.1006/jmsc.2000.0905>, 2000.

- Maneas, G., Makopoulou, E., Bousbouras, D., Berg, H., and Manzoni, S.: Anthropogenic changes in a Mediterranean coastal wetland during the last century – the case of Gialova lagoon, Messinia, Greece, *Water*, 11, 1–22, 2019.
- Manzoni, S., Maneas, G., Scaini, A., Psiloglou, B. E., Destouni, G., and Lyon, S. W.: Hydrology and water quality data from the Gialova lagoon, Greece, 2016–2018, Dataset version 1.0, Bolin Centre Database, <https://doi.org/10.17043/manzoni-2020>, 2020.
- Martinez-Alvarez, V., Gallego-Elvira, B., Maestre-Valero, J. F., and Tanguy, M.: Simultaneous solution for water, heat and salt balances in a Mediterranean coastal lagoon (Mar Menor, Spain), *Estuar. Coast. Shelf Sci.*, 91, 250–261, <https://doi.org/10.1016/j.ecss.2010.10.030>, 2011.
- McMahon, T. A., Peel, M. C., Lowe, L., Srikanthan, R., and McVicar, T. R.: Estimating actual, potential, reference crop and pan evaporation using standard meteorological data: a pragmatic synthesis, *Hydrol. Earth Syst. Sci.*, 17, 1331–1363, <https://doi.org/10.5194/hess-17-1331-2013>, 2013.
- National Observatory of Athens: Methoni actinometric and meteorological station on-line information available at: [http://www.meteo.noa.gr/WeatherOnline/s\\_Methoni/meteo\\_tableEN.html](http://www.meteo.noa.gr/WeatherOnline/s_Methoni/meteo_tableEN.html), last access: 1 July 2019.
- Newton, A., Icely, J., Cristina, S., Brito, A., Cardoso, A. C., Colijn, F., Riva, S. D., Gertz, F., Hansen, J. W., Holmer, M., Ivanova, K., Leppakoski, E., Canu, D. M., Mocenni, C., Mudge, S., Murray, N., Pejrup, M., Razinkovas, A., Reizopoulou, S., Perez-Ruzafa, A., Schernewski, G., Schubert, H., Carr, L., Solidoro, C., Pierluigi Viaroli, and Zaldivar, J. M.: An overview of ecological status, vulnerability and future perspectives of European large shallow, semi-enclosed coastal systems, lagoons and transitional waters, *Estuar. Coast. Shelf Sci.*, 140, 95–122, <https://doi.org/10.1016/j.ecss.2013.05.023>, 2014.
- Obrador, B., Moreno-Ostos, E., and Pretus, J. L.: A Dynamic model to simulate water level and salinity in a Mediterranean coastal lagoon, *Estuar. Coasts*, 31, 1117–1129, <https://doi.org/10.1007/s12237-008-9084-1>, 2008.
- Pantazis, C.: Ecosystem services and groundwater quality: the case study of Gialova Lagoon, MSc thesis, National Technical University of Athens, Metsovion Interdisciplinary Research Center, Athens, 71 pp., 2019.
- Perez-Ruzafa, A., Marcos, C., and Perez-Ruzafa, I. M.: Mediterranean coastal lagoons in an ecosystem and aquatic resources management context, *Phys. Chem. Earth*, 36, 160–166, <https://doi.org/10.1016/j.pce.2010.04.013>, 2011.
- Priestley, C. H. B. and Taylor, R. J.: Assessment of surface heat flux and evaporation using large-scale parameters, *Mon. Weather Rev.*, 100, 81–92, 1972.
- Rodellas, V., Stieglitz, T. C., Andrisoa, A., Cook, P. G., Raimbault, P., Tamborski, J. J., van Beek, P., and Radakovitch, O.: Groundwater-driven nutrient inputs to coastal lagoons: The relevance of lagoon water recirculation as a conveyor of dissolved nutrients, *Sci. Total Environ.*, 642, 764–780, <https://doi.org/10.1016/j.scitotenv.2018.06.095>, 2018.
- Rosenberry, D. O., Winter, T. C., Buso, D. C., and Likens, G. E.: Comparison of 15 evaporation methods applied to a small mountain lake in the northeastern USA, *J. Hydrol.*, 340, 149–166, <https://doi.org/10.1016/j.jhydrol.2007.03.018>, 2007.
- Shuttleworth, W. J.: *Terrestrial Hydrometeorology*, Wiley-Blackwell, Oxford, UK, 2012.
- Stumpp, C., Ekdal, A., Gönenc, I. E., and Maloszewski, P.: Hydrological dynamics of water sources in a Mediterranean lagoon, *Hydrol. Earth Syst. Sci.*, 18, 4825–4837, <https://doi.org/10.5194/hess-18-4825-2014>, 2014.
- Thorslund, J., Jarsjo, J., Jaramillo, F., Jawitz, J. W., Manzoni, S., Basu, N. B., Chalov, S. R., Cohen, M. J., Creed, I. F., Goldenberg, R., Hylin, A., Kalantari, Z., Koussis, A. D., Lyon, S. W., Mazi, K., Mard, J., Persson, K., Pietro, J., Prieto, C., Quin, A., Van Meter, K., and Destouni, G.: Wetlands as large-scale nature-based solutions: Status and challenges for research, engineering and management, *Ecol. Eng.*, 108, 489–497, <https://doi.org/10.1016/j.ecoleng.2017.07.012>, 2017.
- Vigouroux, G., Destouni, G., Jonsson, A., and Cvetkovic, V.: A scalable dynamic characterisation approach for water quality management in semi-enclosed seas and archipelagos, *Mar. Poll. Bull.*, 139, 311–327, <https://doi.org/10.1016/j.marpolbul.2018.12.021>, 2019.
- Weiberg, E., Unkel, I., Kouli, K., Holmgren, K., Avramidis, P., Bonnier, A., Dibble, F., Finne, M., Izdebski, A., Katrantsiotis, C., Stocker, S. R., Andwing, M., Baika, K., Boyd, M., and Heymann, C.: The socio-environmental history of the Peloponnese during the Holocene: Towards an integrated understanding of the past, *Quaternary Sci. Rev.*, 136, 40–65, <https://doi.org/10.1016/j.quascirev.2015.10.042>, 2016.
- Williams, W.: Conductivity and salinity of Australian salt lakes, *Mar. Freshwater Res.*, 37, 177–182, <https://doi.org/10.1071/MF9860177>, 1986.